

Oxidative addition of methyl iodide to $[\text{Rh}(\text{CO})_2\text{I}]_2$: synthesis, structure and reactivity of neutral rhodium acetyl complexes, $[\text{Rh}(\text{CO})(\text{NCR})(\text{COMe})\text{I}_2]_2$ [☆]

Anthony Haynes ^{*}, Peter M. Maitlis, Ian A. Stanbridge, Susanne Haak, Jean M. Pearson, Harry Adams, Neil A. Bailey

Department of Chemistry, University of Sheffield, Dainton Building, Brook Hill, Sheffield S3 7HF, UK

Received 16 February 2004; accepted 13 March 2004

Available online 27 April 2004

Abstract

Reaction of $[\text{Rh}(\text{CO})_2\text{I}]_2$ (**1**) with MeI in nitrile solvents gives the neutral acetyl complexes, $[\text{Rh}(\text{CO})(\text{NCR})(\text{COMe})\text{I}_2]_2$ (R = Me, **3a**; ^tBu, **3b**; vinyl, **3c**; allyl, **3d**). Dimeric, iodide-bridged structures have been confirmed by X-ray crystallography for **3a** and **3b**. The complexes are centrosymmetric with approximate octahedral geometry about each Rh centre. The iodide bridges are asymmetric, with Rh–(μ -I) *trans* to acetyl longer than Rh–(μ -I) *trans* to terminal iodide. In coordinating solvents, **3a** forms mononuclear complexes, $[\text{Rh}(\text{CO})(\text{sol})_2(\text{COMe})\text{I}_2]$ (sol = MeCN, MeOH). Complex **3a** reacts with pyridine to give $[\text{Rh}(\text{CO})(\text{py})(\text{COMe})\text{I}_2]_2$ and $[\text{Rh}(\text{CO})(\text{py})_2(\text{COMe})\text{I}_2]$ and with chelating diphosphines to give $[\text{Rh}(\text{Ph}_2\text{P}(\text{CH}_2)_n\text{PPh}_2)(\text{COMe})\text{I}_2]$ ($n = 2, 3, 4$). Addition of MeI to $[\text{Ir}(\text{CO})_2(\text{NCMe})\text{I}]$ is two orders of magnitude slower than to $[\text{Ir}(\text{CO})_2\text{I}_2]^-$. A mechanism for the reaction of **1** with MeI in MeCN is proposed, involving initial bridge cleavage by solvent to give $[\text{Rh}(\text{CO})_2(\text{NCMe})\text{I}]$ and participation of the anion $[\text{Rh}(\text{CO})_2\text{I}_2]^-$ as a reactive intermediate. The possible role of neutral Rh(III) species in the mechanism of Rh-catalysed methanol carbonylation is discussed.

© 2004 Elsevier B.V. All rights reserved.

Keywords: Rhodium; Iridium; Carbonyl; Iodide; Mechanism; Catalysis

1. Introduction

The carbonylation of methanol to acetic acid is one of the most important applications of homogeneous transition metal catalysis [1–3]. The rhodium/iodide-based process originally developed by Monsanto [4] has recently been superseded on some plants by the iridium/iodide based Cativa process commercialised by BP Chemicals [5–8]. Mechanistic studies have shown that oxidative addition of methyl iodide to the anionic $[\text{Rh}(\text{CO})_2\text{I}_2]^-$ is rate determining in the Rh system and that migratory CO insertion in $[\text{Rh}(\text{CO})_2\text{I}_3\text{Me}]^-$ is rel-

atively fast [9–12]. In the Ir system MeI oxidative addition to $[\text{Ir}(\text{CO})_2\text{I}_2]^-$ is >100 times faster than for the Rh analogue and $[\text{Ir}(\text{CO})_2\text{I}_3\text{Me}]^-$ is the catalyst resting state [13–15]. Carbonylation of $[\text{Ir}(\text{CO})_2\text{I}_3\text{Me}]^-$ is rate controlling, and occurs via substitution of an iodide ligand by CO to give $[\text{Ir}(\text{CO})_3\text{I}_2\text{Me}]$ [16]. Migratory CO insertion in this neutral complex is much faster than in the anionic precursor, and high rates are achieved in the catalytic system by addition of promoters which bind ionic iodide [17].

Although the accepted mechanism for the Rh-based system is dominated by anionic complexes, the potential participation of neutral intermediates can be considered. In this paper, we report an investigation of the reactivity of MeI with the neutral rhodium dimer, $[\text{Rh}(\text{CO})_2\text{I}]_2$ and its monomeric derivatives and describe the synthesis, structure and reactivity of some neutral rhodium acetyl complexes. Based upon these observations, we

[☆] Supplementary data associated with this article can be found, in the online version, at [doi:10.1016/j.ica.2004.03.018](https://doi.org/10.1016/j.ica.2004.03.018).

^{*} Corresponding author. Tel.: +44-114-2229326; fax: +44-114-2229346.

E-mail address: a.haynes@sheffield.ac.uk (A. Haynes).

comment on the possible participation of neutral species in rhodium catalysed methanol carbonylation.

2. Results and discussion

The reactivity of $[\text{Rh}(\text{CO})_2\text{I}]_2$ (**1**) with MeI is solvent dependent. In solvents of low polarity such as CH_2Cl_2 or even neat MeI, a very slow reaction is observed. The dark red-brown solid obtained on removal of the solvent is very air sensitive and only stable under an inert atmosphere for a few hours. The product, **2**, exhibits a terminal $\nu(\text{CO})$ band at 2084 cm^{-1} and low frequency absorptions at 1739 and 1727 cm^{-1} , indicating the presence of an acetyl ligand. Full characterisation of **2** was hindered by its instability although microanalytical data suggest formulation as $[\text{Rh}(\text{CO})(\text{COMe})\text{I}_2]_n$. Further support for this suggestion is provided by the reaction of **2** with Bu_4NI (1 molar equiv/Rh) in CH_2Cl_2 , which gives the known anionic acetyl complex, $[\text{Rh}(\text{CO})(\text{COMe})\text{I}_3]_2^{2-}$ ($\nu(\text{CO})$ 2065s , 1737m and 1717sh cm^{-1}) [18,19].

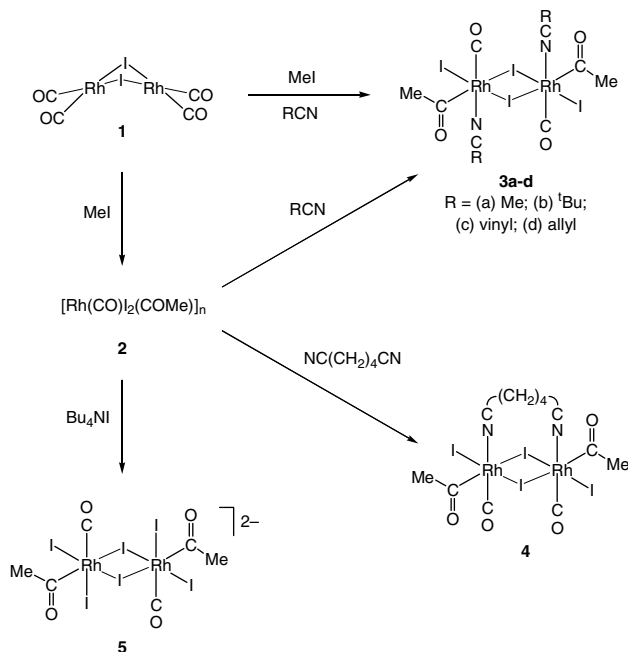
The reaction of **1** with MeI occurs much more readily in nitrile solvents, giving stable products amenable to isolation as solids and detailed characterisation. Spectroscopic and analytical data are consistent with formulation of the products as $[\text{Rh}(\text{CO})(\text{NCR})(\text{COMe})\text{I}_2]_n$ (**3a**, R = Me; **3b**, R = ^tBu; **3c**, R = CH=CH₂; **3d**, R = CH₂CH=CH₂) as shown in Scheme 1. Single-crystal X-ray structure determinations for complexes **3a** and **3b** show them to be dimeric in the solid state with rhodium–iodide bridges (*vide infra*). Complexes **3a–d** could also be prepared by addition of the appropriate nitrile (1

equiv per Rh) to the unstable species **2**, described above. This lends support to the formulation of **2** as $[\text{Rh}(\text{CO})(\text{COMe})\text{I}_2]_n$, which is stabilised upon coordination of nitrile. Solid-state IR spectra of **3a** (as Nujol mulls) were found to be dependent upon the method of isolation. Whereas samples recrystallised from CH_2Cl_2 or MeCN had $\nu(\text{CO})$ bands at 2078 and 1718 cm^{-1} , samples formed by removal of CH_2Cl_2 solvent in *vacuo* displayed bands at 2086 and 1709 cm^{-1} . This may indicate the existence of different isomers of **3a**.

Addition of adiponitrile (0.5 equiv per Rh) to **2** gave a product, **4**, formulated as $[\text{Rh}(\text{CO})(\text{NC}(\text{CH}_2)_4\text{CN})(\text{COMe})\text{I}_2]_n$. The nuclearity of **4** is uncertain, the complex being insufficiently soluble for molecular weight measurements to be carried out. A possible dinuclear structure with the adiponitrile ligand bridging the two Rh centres is shown in Scheme 1.

2.1. X-ray crystallographic structure determinations of $[\text{Rh}(\text{CO})(\text{NCMe})(\text{COMe})\text{I}_2]_2$ (**3a**) and $[\text{Rh}(\text{CO})(\text{NC}^t\text{Bu})(\text{COMe})\text{I}_2]_2$ (**3b**)

The molecular structures of **3a** and **3b** determined by X-ray crystallography are illustrated in Figs. 1 and 2; selected bond lengths and angles are listed in Table 1. The molecules are very similar in structure, each comprising a centrosymmetric, di-iodo-bridged di-rhodium complex. Terminal iodo and acetyl ligands lie *trans* to the bridging iodides. The octahedral coordination sphere about each rhodium is completed by mutually *trans*-carbonyl and nitrile ligands. The nitrile ligands of **3a** and **3b** are slightly bent at the coordinating nitrogen (173° and 167° , respectively) and are approximately linear at the carbon of the cyano group (178° and 174° , respectively). The only significant deviation from ideal octahedral coordination geometry involves the nitrile ligand which bends away from the acetyl ligand, towards the relatively *trans* bridging iodide by 5° (**3a**) or 7° (**3b**). The carbonyl ligands are almost linear. The plane of the acetyl ligand is inclined to the “equatorial” plane of the Rh



Scheme 1. Reactions of **1** leading to Rh(III) acetyl complexes.

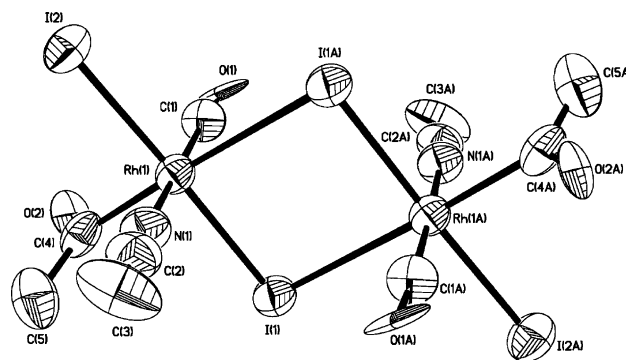


Fig. 1. ORTEP plot (50% probability ellipsoids) for $[\text{Rh}(\text{CO})(\text{NCMe})(\text{COMe})\text{I}_2]_2$ (**3a**). Hydrogen atoms are omitted for clarity.

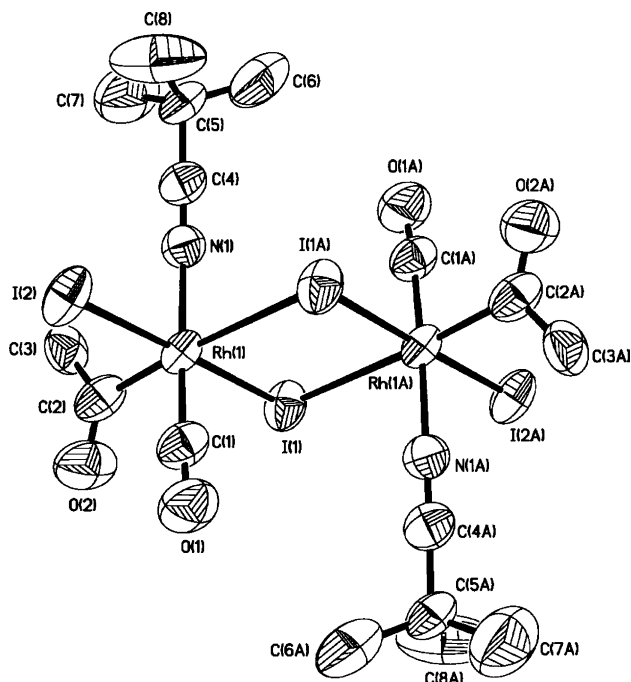


Fig. 2. ORTEP plot (50% probability ellipsoids) for $[\text{Rh}(\text{CO})(\text{NC}'\text{Bu})(\text{COMe})\text{I}_2]_2$ (**3b**). Hydrogen atoms are omitted for clarity.

Table 1
Selected bond lengths (Å) and bond angles (°) for **3a** and **3b**

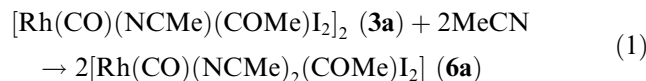
	3a	3b
Rh(1)–I(1)	2.673(2)	2.682(8)
Rh(1)–I(2)	2.652(2)	2.656(8)
Rh(1)–I(1A)	2.960(2)	3.057(9)
Rh(1)–C(1)	1.892(13)	1.854(24)
Rh–C (acetyl)	2.067(13)	2.037(21)
Rh–N(1)	2.089(11)	2.094(20)
C(1)–O(1)	1.071(17)	1.153(29)
C–O (acetyl)	1.179(18)	1.213(32)
C–C (acetyl)	1.433(22)	1.474(28)
N–C (nitrile)	1.116(19)	1.174(30)
C–C (nitrile)	1.438(22)	1.472(31)
Rh(1)···Rh(1A)	4.053(3)	4.159(3)
I(1)–Rh(1)–I(2)	177.0(1)	178.8(2)
N(1)–Rh(1)–C(1)	174.1(5)	174.1(7)
C(acetyl)–Rh(1)–I(1A)	176.5(3)	176.4(6)
I(1)–Rh(1)–I(1A)	88.1(1)	87.3(2)
I(2)–Rh(1)–C(acetyl)	88.6(3)	89.4(6)
I(2)–Rh(1)–N(1)	89.6(2)	88.9(4)
I(2)–Rh(1)–C(1)	87.9(3)	88.2(6)
I(2)–Rh(1)–I(1A)	94.5(1)	93.1(2)
N(1)–Rh(1)–C(acetyl)	95.1(5)	96.9(8)
N(1)–Rh(1)–I(1A)	86.6(3)	85.8(4)
Rh(1)–I(1)–Rh(1A)	91.9(1)	92.7(2)
Rh(1)–C(1)–O(1)	176.7(12)	176.1(18)
Rh(1)–C–O (acetyl)	118.7(10)	121.1(14)
Rh(1)–C–C (acetyl)	115.5(10)	117.6(17)
Rh(1)–N(1)–C (nitrile)	172.5(11)	167.4(15)
N(1)–C–C (nitrile)	178.0(14)	173.8(20)

by 82° (**3a**) or 81° (**3b**). The two mutually *trans*-Rh–I bonds (one terminal, one bridging) are very similar in length (2.65–2.68 Å in both complexes) but the other Rh–(μ-I) distance is much longer (2.96 Å, **3a**; 3.06 Å, **3b**), reflecting the strong *trans* influence of the acetyl ligand. The non-bonded Rh···Rh distance is longer for **3b** (4.16 Å) than for **3a** (4.05 Å), presumably due to the bulky ^tBuCN ligands. There are no significant intermolecular contacts for either complex.

The structure most closely related to those determined here is that of the dianion, $[\text{Rh}(\text{CO})(\text{COMe})\text{I}_3]_2^{2-}$ (**5**), isolated as its Me_3PhN^+ salt by Forster and co-workers [18]. Our neutral complexes **3a** and **3b** are formally derived from the dianion by substitution of two terminal iodide ligands *trans* to carbonyls by the appropriate nitrile. The principal features of the crystal structure of **5** are very similar to those of **3a** and **3b**. All three complexes show distinct asymmetry in the Rh(μ-I)₂Rh unit. In each case the Rh–(μ-I) bond *trans* to acetyl is substantially (0.29–0.37 Å) longer than the Rh–(μ-I) bond *trans* to iodide due to the strong *trans* influence of acetyl.

2.2. Solution behaviour of $[\text{Rh}(\text{CO})(\text{NCMe})(\text{COMe})\text{I}_2]_2$ (**3a**)

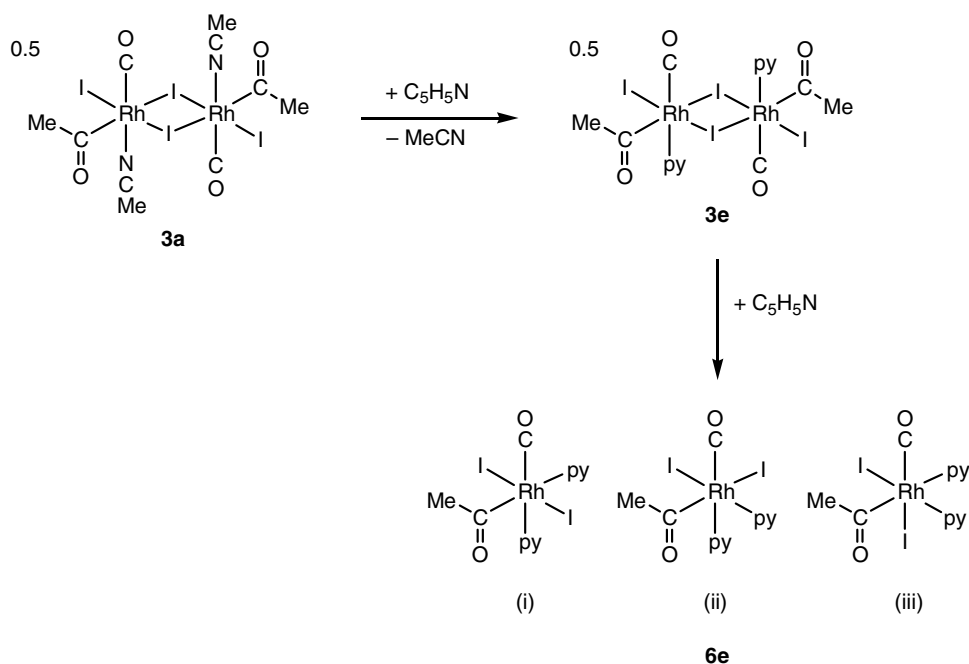
Vapour phase osmometry measurements gave molecular weights of 802 and 474 for solutions of **3a** in CHCl_3 and MeCN, respectively. The dimer identified by X-ray crystallography has a molecular weight of 937.64. The results therefore indicate that **3a** remains predominantly dimeric in CHCl_3 , but is cleaved to mononuclear species in MeCN. The IR spectra of **3a** in CHCl_3 or CH_2Cl_2 exhibit shoulders on both terminal and acetyl $\nu(\text{CO})$ bands. Similar features have previously been observed for the dianion, **5**, and were explained by the presence of a mixture of dimeric isomers in solution [20]. Addition of MeCN to a solution of **3a** in CHCl_3 resulted in band shifts from 2090 (2075sh) and 1733 (1740sh) cm^{-1} to 2096 (2084sh) and 1718 cm^{-1} . The ¹H NMR of **3a** in CDCl_3 shows broad signals due to the acetyl and MeCN ligands at δ 2.88 and 2.62. Addition of MeCN (20 equiv/**3a**) resulted in sharpening of both resonances and small shifts to δ 2.86 and 2.60, together with the growth of a signal at δ 2.00 due to free MeCN. Subsequent addition of CD_3CN (excess) caused the disappearance of the signal at 2.20, due to displacement of coordinated CH_3CN at the Rh centre. The spectroscopic data do not reveal the precise structure(s) of the species generated by addition of MeCN to **3a**, but are consistent with cleavage of the dimer to give $[\text{Rh}(\text{CO})(\text{NCMe})_2(\text{COMe})\text{I}_2]$, **6a** (Eq. (1)). Complex **6a** was never isolated from solution; crystallisation always lead to the dimer, **3a**



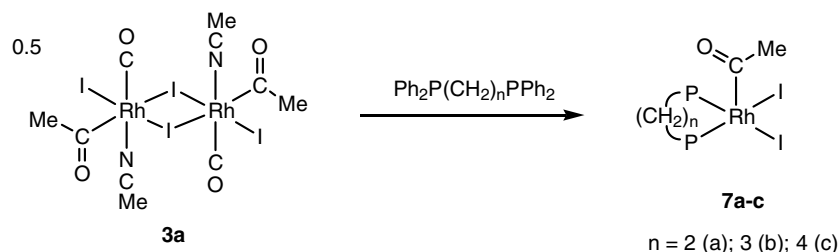
2.3. Pyridine adducts

Addition of pyridine (2 equiv) to **3a** resulted in isolation of a product formulated as $[\text{Rh}(\text{CO})(\text{py})(\text{COMe})\text{I}_2]_n$, **3e**. It is likely that this complex has a similar dimeric structure to **3a**, resulting from substitution of the MeCN ligands by the more strongly coordinating pyridine. The same product was also synthesised by addition of pyridine (1 equiv/Rh) to **2**. A one-pot synthesis of **3e** by oxidative addition of MeI to **1** in the presence of pyridine is precluded by the facile quaternisation of pyridine under these conditions, leading to ionic products.

Addition of 2 molar equivalents (per Rh) of pyridine to **3a** (or 1 equiv/Rh to **3e**) gave $[\text{Rh}(\text{CO})(\text{py})_2(\text{COMe})\text{I}_2]$ (**6e**) which exhibits unshouldered IR absorptions in both the terminal and acetyl $\nu(\text{CO})$ regions, suggesting a single isomer. The ^1H NMR spectrum indicates the presence of inequivalent pyridine ligands; three possible structures are shown in Scheme 2. We favour structures (i) or (ii) by analogy with $[\text{Rh}(\text{CO})(\text{py})(\text{COMe})\text{I}_3]^-$, which contains a pyridine ligand *trans* to CO [20].



Scheme 2. Formation of pyridine adducts including possible isomers of **6e**.



Scheme 3. Reaction of **3a** with diphosphines.

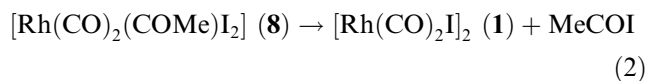
2.4. Reactions of $[\text{Rh}(\text{CO})(\text{NCMe})(\text{COMe})\text{I}_2]_2$ (**3a**) with diphosphines

Complex **3a** was found to be a useful starting material for preparation of other neutral Rh(III) acetyl complexes. For example, treatment of **3a** with chelating diphosphines results in loss of MeCN and CO ligands to yield the monomers $[\text{Rh}(\text{Ph}_2\text{P}(\text{CH}_2)_n\text{PPh}_2)(\text{COMe})\text{I}_2]$ ($n = 2-4$; **7a-c**, Scheme 3).

The dppe and dppp complexes (**7a** and **7b**, respectively) were first isolated in a study of the rhodium/iodide catalysed reductive carbonylation of methanol, and **7c** can also be prepared by the stoichiometric reaction of $[\text{Rh}(\text{CO})(\text{dppe})\text{I}]$ with MeI [21,22]. Crystal structures reported for **7a** [22], **7b** [23,24] (and also the dppm analogue [25]) show these complexes to adopt an approximate square pyramidal geometry with an apical acetyl ligand. The dppb derivative, **7c**, which has not previously been reported, shows a doublet (δ 72.1, $^1J_{\text{Rh-P}}$ 136 Hz) for equivalent phosphorus atoms in its ^{31}P NMR spectrum and likely has an analogous structure.

2.5. Reaction of $[\text{Rh}(\text{CO})(\text{NCMe})(\text{COMe})\text{I}_2]_2$ (**3a**) with CO

Brief bubbling of solutions of **3a** in CH_2Cl_2 with CO results in the formation of a new species (**8**) with $\nu(\text{CO})$ bands at 2154_{vw} 2102_s and 1733_m cm^{-1} as well as free MeCN ($\nu(\text{CN})$ 2255 cm^{-1}). The IR spectrum of **8** resembles that of *trans*- $[\text{Rh}(\text{CO})_2(\text{COMe})\text{I}_3]^-$ ($\nu(\text{CO})$: 2141, 2084, 1706 cm^{-1}) [19] but with each absorption shifted to higher frequency, as expected for a neutral complex compared to an anion. The data are consistent with **8** having the formula $[\text{Rh}(\text{CO})_2(\text{COMe})\text{I}_2]_n$, which is formally derived from $[\text{Rh}(\text{CO})_2(\text{COMe})\text{I}_3]^-$ by removal of an iodide ligand. However, we cannot distinguish between monomeric and dimeric structures for **8**. The $\nu(\text{CO})$ bands of **8** decay completely within ca. 30 min at 25 °C (much faster than decomposition of $[\text{Rh}(\text{CO})_2(\text{COMe})\text{I}_3]^-$ [19]) and new absorptions assigned to the Rh(I) dimer **1** grow at 2096, 2080 and 2026 cm^{-1} . The conversion of **8** into **1** requires the formal reductive elimination of acetyl iodide



The organic product was not directly observed, probably due to hydrolysis to acetic acid and HI by traces of adventitious water. Consistent with this, $\nu(\text{CO})$ bands at 2071 and 2003 cm^{-1} revealed the presence of small amounts of $\text{H}[\text{Rh}(\text{CO})_2\text{I}]$ formed by reaction of **1** with HI [26]. By contrast, no change in the IR spectrum is observed on bubbling CO through solutions of **3a** in donor solvents such as MeCN or MeOH. The Rh-containing species present under these conditions is a monomeric bis(solvate), $[\text{Rh}(\text{CO})(\text{COMe})\text{I}_2(\text{sol})_2]$ and coordination of a second CO ligand is inhibited by a large excess of coordinating solvent.

2.6. Iodide coordination/dissociation

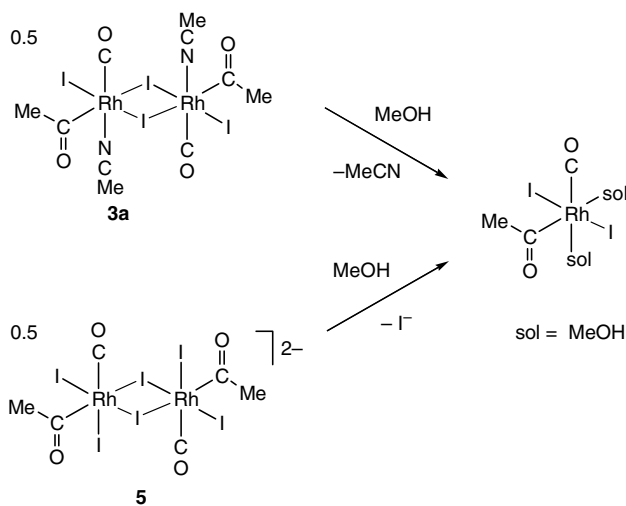
The IR spectra of **3a** and **5** in CH_2Cl_2 showed the expected differences between a neutral and an anionic complex. Thus, the terminal $\nu(\text{CO})$ band of **3a** is ca. 25 cm^{-1} higher in frequency than that of **5**, a shift which is ascribed to decreased π -backbonding in the neutral species. Addition of a stoichiometric quantity of Bu_4NI to a solution of **3a** in CH_2Cl_2 resulted in shifts of the $\nu(\text{CO})$ bands to low frequency, consistent with coordination of iodide. On addition of an additional equivalent of Bu_4NI , the broad, shouldered absorptions of **5** were replaced by narrower, more symmetrical bands in both terminal and acetyl $\nu(\text{CO})$ regions. Addition of excess Bu_4NI caused no further modifications. These spectral changes are consistent with bridge cleavage of **5** by iodide anion, to give the di-anionic tetraiodide

complex, $[\text{Rh}(\text{CO})(\text{COMe})\text{I}_4]^{2-}$ (**9**). Our data do not define the stereochemistry of **9** (which is related to the known dianion $[\text{Rh}(\text{CO})\text{I}_5]^{2-}$ [27]) but a structure with carbonyl *cis* to acetyl (as in **5**) is considered likely.

Significantly different behaviour was observed in MeOH, in which solutions of **3a** or **5** display remarkably similar $\nu(\text{CO})$ frequencies. Both exhibit split absorptions in the terminal and acetyl regions (2077, 2066, 1742, 1726 cm^{-1}) with only very slight differences in the relative intensities of the component bands. The spectra suggest formation of the same species from the neutral or anionic precursor in MeOH solution. We propose that bridge cleavage, accompanied by loss of MeCN from **3a** or I^- from **5** leads to a bis(solvate) complex, $[\text{Rh}(\text{CO})(\text{MeOH})_2(\text{COMe})\text{I}_2]$ (Scheme 4).

Addition of a stoichiometric quantity of AgBF_4 to a methanolic solution of **5** leads to precipitation of silver iodide but no discernible change in the IR spectrum. Therefore, the same Rh complex is present before and after precipitation of iodide, demonstrating that iodide dissociation occurs when **5** is dissolved in MeOH. Similarly, mixing equimolar methanolic solutions of **3a** and **1** resulted in formation of $[\text{Rh}(\text{CO})_2\text{I}_2]^-$ (by reaction of **1** with I^-) but no change in the IR bands of the Rh(III) acetyl species. This result demonstrates that Rh(I) has a higher affinity for I^- than Rh(III).

In pyridine, the IR spectra of **3a** or **5** indicated the presence of $[\text{Rh}(\text{CO})(\text{py})_2(\text{COMe})\text{I}_2]$ (**6e**), whereas in MeCN or *i*PrOH, the spectra were more complex and varied with the iodide concentration, suggesting an equilibrium mixture of neutral and anionic complexes. This can be explained by the weaker coordinating power of MeCN (compared to pyridine) and the poorer anion-solvating ability of *i*PrOH, compared to MeOH.

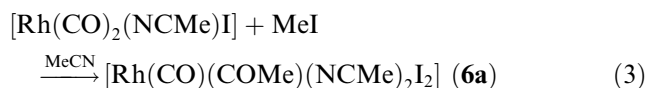


Scheme 4. Formation of bis(solvate) complexes from **3a** and **5**. (Stereochemistry of product uncertain.)

2.7. Mechanism of reaction of $[\text{Rh}(\text{CO})_2(\text{NCMe})\text{I}]_2$ with MeI

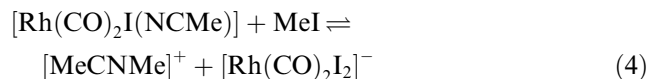
Solutions of **1** in CH_2Cl_2 exhibit two strong $\nu(\text{CO})$ bands at 2080 and 2027 cm^{-1} as well as a third band of medium intensity at 2096 cm^{-1} , consistent with a non-planar dimeric structure for **1** analogous to the solid-state structure of $[\text{Rh}(\text{CO})_2\text{Cl}]_2$ [28]. In MeCN solution, however, only two $\nu(\text{CO})$ bands are observed at 2088 and 2023 cm^{-1} . Addition of small amounts of MeCN to a CH_2Cl_2 solution of **1** resulted in the smooth conversion of the three-band spectrum into the two-band spectrum. Analogous spectroscopic observations have been reported for addition of MeCN to $[\text{Rh}(\text{CO})_2\text{Cl}]_2$ in CHCl_3 [29]. On the basis of the disappearance of the high frequency $\nu(\text{CO})$ band and the lack of a $\nu(\text{CN})$ band for coordinated MeCN, it was suggested that $[\text{Rh}(\text{CO})_2\text{Cl}]_2$ becomes planar (with the A_1 $\nu(\text{CO})$ mode becoming IR inactive). In our studies, however, we have detected weak $\nu(\text{CN})$ absorptions (2328 cm^{-1} , X = Cl; 2327 cm^{-1} , X = I) on addition of small quantities of MeCN to $[\text{Rh}(\text{CO})_2\text{X}]$ in CHCl_3 . This is consistent with coordination of MeCN and cleavage of the halide bridges to give monomeric *cis*- $[\text{Rh}(\text{CO})_2(\text{NCMe})\text{X}]$. Vapour phase osmometry measurements gave molecular weights for solutions of **1** as 596 (CHCl_3) and 274 (MeCN), indicating retention of the dimeric structure in CHCl_3 but complete conversion to a monomer in MeCN. Other nitriles are known to cleave $[\text{Rh}(\text{CO})_2\text{X}]_2$ (X = Cl, Br) to give stable products [30], but attempts to isolate $[\text{Rh}(\text{CO})_2(\text{NCMe})\text{X}]$ from solution were unsuccessful. We note that $[\text{Rh}(\text{CO})_2\text{Cl}]_2$ is also known to undergo bridge cleavage by MeOH to give *cis*- $[\text{Rh}(\text{CO})_2(\text{MeOH})\text{Cl}]$ [31].

During the reaction with MeI (3.2 M in MeCN), the IR absorptions of $[\text{Rh}(\text{CO})_2(\text{NCMe})\text{I}]$ decay and are replaced by bands at 2091 and 1713 cm^{-1} due to **6a**



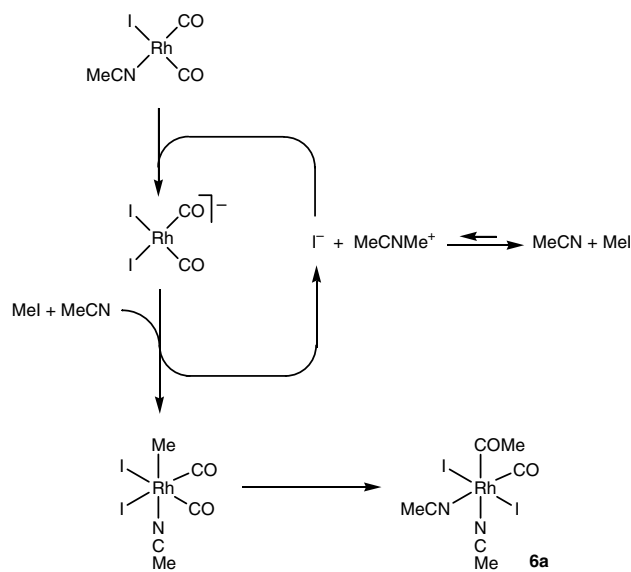
Plots of absorbance against time for both the reactant band at 2023 cm^{-1} and the product band at 1713 cm^{-1} are approximately linear, indicating that the reaction is zeroth-order in $[\text{Rh}(\text{CO})_2(\text{NCMe})\text{I}]$. This contrasts with the reactions of most square planar complexes with MeI, which are first order in complex [12,22,32]. The kinetic data indicate that the rate determining step of Eq. (3) is *not* a direct bimolecular reaction between $[\text{Rh}(\text{CO})_2(\text{NCMe})\text{I}]$ and MeI. On close inspection of the IR spectra, additional weak absorptions are present at 2058 and 1984 cm^{-1} , which grow at the start of the reaction and then decay away. These absorptions exactly match those of $[\text{Rh}(\text{CO})_2\text{I}_2]^-$ in MeCN and indicate that the anion participates as an intermediate in the reaction.

Formation of $[\text{Rh}(\text{CO})_2\text{I}_2]^-$ requires a source of iodide anion. The possibility of redistribution of iodide and MeCN ligands between Rh centres is ruled out by the absence of $\nu(\text{CO})$ bands due to the known cation $[\text{Rh}(\text{CO})_2(\text{NCMe})_2]^+$ [33]. The only other source of iodide is from the excess MeI present. It is known that N-methylation of MeCN can be achieved using strong methylating agents such as $[\text{Me}_3\text{O}]\text{BF}_4$ or by using alkyl halides in the presence of a halide acceptor (e.g. SbCl_5) [34]. By analogy, in our system, the Rh centre can act as an iodide acceptor to facilitate formation of the dimethylnitrilium cation



Although this equilibrium will favour the neutral reactants, it is feasible that a small concentration of $[\text{Rh}(\text{CO})_2\text{I}_2]^-$ can accumulate. We did not detect $[\text{MeCNMe}]^+$ directly, and it is possible that hydrolysis by adventitious water occurs to give the amide, MeC(O)NHMe and H^+ , which could then act as counter-ion for $[\text{Rh}(\text{CO})_2\text{I}_2]^-$. This anion is expected to be more nucleophilic toward MeI than $[\text{Rh}(\text{CO})_2(\text{NCMe})\text{I}]$, as demonstrated for the Ir analogues (vide infra). The rate of the overall reaction with MeI is therefore determined by the concentration of $[\text{Rh}(\text{CO})_2\text{I}_2]^-$ rather than the neutral precursor, resulting in the observed zero-order dependence on $[\text{Rh}(\text{CO})_2(\text{NCMe})\text{I}]$.

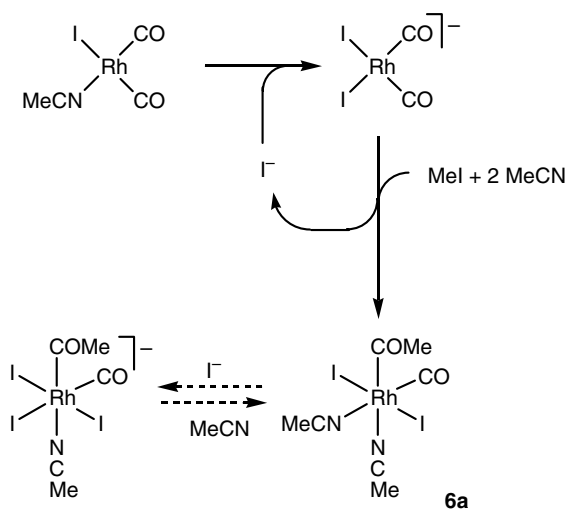
A mechanism consistent with these observations is shown in Scheme 5. Displacement of coordinated solvent from $[\text{Rh}(\text{CO})_2\text{I}(\text{NCMe})]$ by iodide leads to $[\text{Rh}(\text{CO})_2\text{I}_2]^-$. This anion then acts as a nucleophile toward MeI, releasing I^- and forming a neutral Rh(III)–



Scheme 5. Mechanism for reaction of $[\text{Rh}(\text{CO})_2(\text{NCMe})\text{I}]$ with MeI in MeCN. (Stereochemistry of octahedral Rh(III) products uncertain.)

methyl species. At this stage, the I^- released by the S_N2 reaction can coordinate to the Rh(III) centre to give $[Rh(CO)_2I_3Me]^-$ [11,12] or to unreacted Rh(I). The soft I^- is expected to bind preferentially to the lower oxidation state, leading to regeneration of $[Rh(CO)_2I_2]^-$ from $[Rh(CO)_2(NCMe)I]$. Thus, sub-stoichiometric I^- , generated in situ from MeI, acts as a catalyst for the oxidative addition. Similar catalysis by I^- has been reported previously for $[Rh(CO)(ER_3)_2I]$ (E = P, As, Sb) [35]. Migratory CO insertion in the neutral Rh–methyl species (probably solvated by MeCN) would lead to the observed product, **6a**.

Further evidence that I^- can act as a catalyst was provided by experiments in which a 1:1 mixture of $[Rh(CO)_2(NCMe)I]$ and $[Rh(CO)_2I_2]^-$ was used. Unexpectedly, the $\nu(CO)$ bands of the *less* nucleophilic neutral species decayed first, with product bands due to **6a** appearing during this phase of the reaction. Only when this process was close to completion did the $\nu(CO)$ bands of $[Rh(CO)_2I_2]^-$ begin to decay. This result is counter-intuitive but can be explained by the mechanism shown in Scheme 6. Of the two reactant complexes present, MeI is expected to react preferentially with the anion, $[Rh(CO)_2I_2]^-$. As in Scheme 5, the nucleophilic substitution releases I^- which rapidly coordinates to Rh(I) in preference to Rh(III). Thus, a molecule of $[Rh(CO)_2(NCMe)I]$ is converted into $[Rh(CO)_2I_2]^-$, resulting in the observed depletion of $[Rh(CO)_2(NCMe)I]$, whilst the concentration of $[Rh(CO)_2I_2]^-$ remains approximately constant. Only when most of the $[Rh(CO)_2(NCMe)I]$ has reacted does net consumption of $[Rh(CO)_2I_2]^-$ begin. In this latter stage of the reaction, a mixture of neutral and anionic Rh(III) acetyl products is formed according to the equilibrium at the bottom of Scheme 6.



Scheme 6. Mechanism for reaction of $[Rh(CO)_2(NCMe)I]/[Rh(CO)_2I_2]^-$ mixture with MeI.

2.8. Oxidative addition of MeI to $[Ir(CO)_2(NCMe)I]$

Iodide abstraction from $[Ir(CO)_2I_2]^-$ using $AgBF_4$ or InI_3 in the presence of MeCN generates $[Ir(CO)_2(NCMe)I]$ ($\nu(CO)$ 2078, 2006 cm^{-1} ; $\nu(CN)$ 2333 cm^{-1}). Subsequent addition of MeI (excess) leads to conversion into a product with $\nu(CO)$ bands at higher frequency (2125, 2081 cm^{-1}) assigned to $[Ir(CO)_2(NCMe)I_2Me]$. The same species is formed on dissolving $[Ir(CO)_2I_2Me]_2$ in MeCN [17].

The kinetics of oxidative addition were measured by monitoring the decay of the 2006 cm^{-1} absorption band of $[Ir(CO)_2(NCMe)I]$. A good exponential curve fit establishes that the reaction is first order in $[Ir(CO)_2(NCMe)I]$. Pseudo-first-order rate constants (k_{obs}) obtained over a range of MeI concentrations and temperatures are listed in Supporting Material (together with data obtained for $[Ir(CO)_2I_2]^-$ in the same solvent). A linear plot of k_{obs} versus $[MeI]$ demonstrates the reaction to be first order in MeI and therefore second order overall. The effect of removing an iodide ligand is dramatic, the second-order rate constant for addition of MeI to $[Ir(CO)_2(NCMe)I]$ ($1.56 \times 10^{-5} M^{-1} s^{-1}$; 25 °C) being two orders of magnitude smaller than that for $[Ir(CO)_2I_2]^-$ ($1.34 \times 10^{-3} M^{-1} s^{-1}$). Interestingly, the rate constant for *neutral iridium* complex $[Ir(CO)_2(NCMe)I]$ is of a similar magnitude to that for the *anionic rhodium* complex, $[Rh(CO)_2I_2]^-$ ($k_2 = 2.5 \times 10^{-5} dm^3 mol^{-1} s^{-1}$; 25 °C; CH_2Cl_2) [36].

Activation parameters calculated from an Eyring plot of the variable temperature data are $\Delta H^\ddagger = 49 (\pm 3) kJ mol^{-1}$ and $\Delta S^\ddagger = -171 (\pm 11) J mol^{-1} K^{-1}$ for $[Ir(CO)_2I(NCMe)]$ and $\Delta H^\ddagger = 53 (\pm 2) kJ mol^{-1}$ and $\Delta S^\ddagger = -122 (\pm 6) J mol^{-1} K^{-1}$ for $[Ir(CO)_2I_2]^-$. The lower reactivity of $[Ir(CO)_2I(NCMe)]$ appears to be largely due to a more negative ΔS^\ddagger term, perhaps due to stronger solvation of the polar transition state derived from two neutral reactants.

2.9. Participation of neutral complexes in Rh-catalysed methanol carbonylation

Oxidative addition is rate-controlling for Rh-catalysed carbonylation and $[Rh(CO)_2I_2]^-$ is the catalyst resting state observed by in situ IR spectroscopy [9,10]. Model stoichiometric studies show that sequential reaction of $[Rh(CO)_2I_2]^-$ with MeI and CO gives anionic Rh(III) products, but these are not detected in the catalytic regime. As conventionally drawn, the mechanism for the rhodium/iodide catalysed carbonylation of methanol comprises four anionic Rh complexes [2,9,10]. However, it is clear that this is an over-simplification. The MeI oxidative addition step is generally considered to proceed via two steps: (i) S_N2 attack by $[Rh(CO)_2I_2]^-$ on MeI; (ii) coordination of I^- to Rh(III) [37–39]. The neutral intermediate in this process, $([Rh(CO)_2I_2Me])$ or

a solvent coordinated derivative), is not normally included in the catalytic cycle, although its presence is not disputed. The results presented in this paper indicate that migratory CO insertion is facile on a neutral Rh(III) centre, leading to the possibility that this can occur in the catalytic system. In the Ir-catalysed process, the requirement for iodide loss from $[\text{Ir}(\text{CO})_2\text{I}_3\text{Me}]^-$ prior to CO insertion has been established [15–17]. Whilst this step is not rate-determining for the Rh system, it is still possible that migratory insertion occurs in a neutral Rh(III)–methyl species. Theoretical calculations suggest that the activation enthalpy for methyl migration in $[\text{Rh}(\text{CO})_2\text{I}_2\text{Me}]$ is lower than that for $[\text{Rh}(\text{CO})_2\text{I}_3\text{Me}]^-$ by ca. 12 kJ mol⁻¹ [40].

Our results also demonstrate that in polar, coordinating solvents the anionic dimer, $[\text{Rh}(\text{CO})(\text{COMe})\text{I}_3]_2^{2-}$ (**5**) loses I⁻ to give $[\text{Rh}(\text{CO})(\text{sol})_2(\text{COMe})\text{I}_2]$ (Scheme 4). Under catalytic conditions (aqueous acetic acid/high temperature) the extent of iodide dissociation from Rh(III) acetyl species could also be significant. The resulting neutral species may undergo more facile reductive elimination, as in other systems where a halide loss mechanism has been demonstrated [41–46]. Indeed, decomposition of $[\text{Rh}(\text{CO})_2(\text{COMe})\text{I}_2]_n$ to Rh(I) species is fast compared with $[\text{Rh}(\text{CO})_2(\text{COMe})\text{I}_3]^-$.

3. Conclusions

As expected, the neutral Rh(I) dimer, $[\text{Rh}(\text{CO})_2\text{I}]$ **1** displays lower reactivity toward MeI than the anionic carbonylation catalyst, $[\text{Rh}(\text{CO})_2\text{I}_2]^-$. Kinetic measurements on related Ir(I) complexes show that addition of MeI to $[\text{Ir}(\text{CO})_2(\text{NCMe})\text{I}]$ is two orders of magnitude slower than to $[\text{Ir}(\text{CO})_2\text{I}_2]^-$. In nitrile solvents, reactions between **1** and MeI lead to stable Rh(III) acetyl products, isolated as the iodide bridged dimers $[\text{Rh}(\text{CO})(\text{NCR})(\text{COMe})\text{I}_2]_2$ (**3a–d**). X-ray structures for the MeCN (**3a**) and ^tBuCN (**3b**) derivatives reveal significant asymmetry in the Rh–(μ-I)–Rh bridges, ascribed to the strong *trans* influence of acetyl. The nitrile ligands of **3a** are easily displaced, for example by pyridine, and reaction with diphosphine ligands leads to $[\text{Rh}(\text{Ph}_2\text{P}(\text{CH}_2)_n\text{PPh}_2)(\text{COMe})\text{I}_2]$ (**7a–c**). In coordinating solvents, the chemistry is dominated by mononuclear complexes. Thus, **1** and **3a** are cleaved in MeCN to give $[\text{Rh}(\text{CO})_2(\text{NCMe})\text{I}]$ and $[\text{Rh}(\text{CO})(\text{NCMe})_2(\text{COMe})\text{I}_2]$, respectively. The reaction of $[\text{Rh}(\text{CO})_2(\text{NCMe})\text{I}]$ with MeI displays kinetics which are zeroth-order in the reactant complex, and IR spectroscopy shows that $[\text{Rh}(\text{CO})_2\text{I}_2]^-$ participates as a reactive intermediate. It is proposed that small amounts of iodide anion (generated from MeCN and MeI) act as a catalyst, with Rh(I) binding I⁻ more strongly than Rh(III). Interestingly, neutral $[\text{Rh}(\text{CO})(\text{sol})_2(\text{COMe})\text{I}_2]$ species are generated from the anion, $[\text{Rh}(\text{CO})(\text{COMe})\text{I}_3]_2^{2-}$ in coordinating solvents. The results raise the possibility that neutral

Rh(III) methyl and acetyl complexes are significant intermediates in Rh-catalysed methanol carbonylation.

4. Experimental

4.1. Materials

All solvents used for synthetic or kinetic experiments were distilled and degassed prior to use the following literature procedures. Synthetic procedures were carried out utilising standard Schlenk techniques. Nitrogen and carbon monoxide were dried through a short (20 × 3 cm diameter) column of molecular sieves (4 Å) which was regularly regenerated. Carbon monoxide was also passed through a short column of activated charcoal to remove any iron pentacarbonyl impurity [47]. The compounds $[\text{Rh}(\text{CO})_2\text{Cl}]_2$ [48], $[\text{Rh}(\text{CO})_2\text{I}]_2$ [36] and $\text{Ph}_4\text{As}[\text{Ir}(\text{CO})_2\text{I}_2]$ [17] were synthesised according to the literature procedures. Methyl iodide (Aldrich) was distilled over calcium hydride and stored in foil-wrapped Schlenk tubes under nitrogen and over mercury to prevent formation of I₂.

4.2. Instrumentation

FT-IR spectra (2 cm⁻¹ resolution) were measured using a Perkin–Elmer 1600 spectrometer or a Mattson Genesis Series spectrometer, controlled by WINFIRST software. ¹H NMR spectra were obtained using a Bruker AM250 or WP80SY spectrometer using the solvent or TMS as internal reference. ³¹P NMR spectra were obtained using a Bruker WP80SY spectrometer using orthophosphoric acid as external reference. Elemental analyses were performed by the University of Sheffield microanalysis service.

4.3. Synthesis of $[\text{Rh}(\text{CO})(\text{COMe})\text{I}_2]_n$ (**2**)

$[\text{Rh}(\text{CO})_2\text{I}]_2$ (**1**) (0.1 g, 0.175 mmol) was dissolved in MeI (15 cm³) under N₂ and stirred at room temperature. The reaction was monitored periodically by IR spectroscopy. When the absorption of **1** at 2023 cm⁻¹ had disappeared, the solution was filtered under nitrogen and the MeI removed in vacuo. The resulting dark brown solid (**2**) was examined by IR spectroscopy and microanalysis; yield: 0.06 g (40%). *Anal. Calc.* for C₃H₃I₂O₂Rh: C, 8.4; H, 0.7; I, 59.3. Found: C, 7.6; H, 0.7; I, 61.5%. IR (CH₂Cl₂), ν(CO)/cm⁻¹: 2084, 1739, 1727.

4.4. Synthesis of $[\text{Rh}(\text{CO})(\text{NCMe})(\text{COMe})\text{I}_2]_2$ (**3a**)

$[\text{Rh}(\text{CO})_2\text{I}]_2$ (**1**) (0.46 g, 0.80 mmol) was dissolved in MeCN/MeI (50 cm³, 2:1 v/v) and stirred at room temperature under N₂ (6 h), whereupon IR spectroscopy indicated the disappearance of **1**. The volatile portion of the solvent was removed in vacuo and the resulting or-

ange precipitate redissolved in the remaining liquor by warming. Cooling the solution to 0 °C gave a crop of dark red crystals which were collected by filtration. After further reduction in vacuo, the filtrate yielded a second crop of crystals as described above. The product was dried in vacuo; crystals were of sufficient quality for an X-ray crystallographic study; yield: 0.66 g (87%). *Anal.* Calc. for $C_5H_6I_2NO_2Rh$: C, 12.8; H, 1.3; N, 3.0; I, 54.1. Found: C, 12.9; H, 1.3; N, 2.5; I, 54.3%. IR (Nujol), $\nu(CO)/cm^{-1}$: 2086, 1709; $\nu(CN)/cm^{-1}$: 2327w, 2299w. 1H NMR (250 MHz, $CDCl_3$): δ 2.88 (3H, br s, $COCH_3$), 2.62 (3H, br s, $NCCCH_3$).

Alternative method: Complex **3a** was also prepared by addition of MeCN (2 cm^3) to a stirred solution of **2** (0.2 g, 0.35 mmol) in CH_2Cl_2 (10 cm^3). After removal of the solvent in vacuo, the product was recrystallised from a minimum volume of warm MeCN. Analytical and spectroscopic data confirmed the product to be identical to a sample of **3a** prepared by the method described above; yield: 0.19 g (87%).

4.5. Synthesis of $[Rh(CO)(COMe)I_2(NC^tBu)]_2$ (**3b**)

$[Rh(CO)_2I_2]$ (**1**) (0.235 g, 0.41 mmol) was dissolved in $tBuCN/MeCN$ (10 cm^3 , 9:1 v/v) and stirred at room temperature under N_2 (8 h). Removal of the volatile portion of the solvent in vacuo gave an orange powder which was collected by filtration. The product was washed with diethyl ether, then dissolved in a minimum volume of warm CH_2Cl_2 and placed in the refrigerator at 0 °C, giving a crop of dark red crystals; yield: 0.385 g (92%). *Anal.* Calc. for $C_8H_{12}I_2NO_2Rh$: C, 18.8; H, 2.4; N, 2.7; I, 49.7. Found: C, 18.8; H, 2.3; N, 2.5; I, 49.5%. IR (Nujol), $\nu(CO)/cm^{-1}$: 2085, 1729; $\nu(CN)/cm^{-1}$: 2286w. 1H NMR (250 MHz, CD_3OD): δ 2.75 ($COCH_3$).

4.6. Synthesis of $[Rh(CO)(COMe)I_2(NCCHCH_2)]_2$ (**3e**)

$[Rh(CO)_2I_2]$ (**1**) (0.5 g, 0.87 mmol) was dissolved in acrylonitrile/MeI (10 cm^3 , 5:1 v/v) and stirred at room temperature under N_2 (48 h). Removal of the solvent in vacuo gave an orange powder which was recrystallised from a minimum volume of warm CH_2Cl_2 to give orange microcrystals of **3e**. Concentration of the solution and recrystallisation at -36 °C gave a further crop of crystals; yield: 0.702 g (83%). *Anal.* Calc. for $C_6H_6I_2NO_2Rh$: C, 15.0; H, 1.3; N, 2.9; I, 52.8. Found: C, 15.0; H, 1.3; N, 2.6; I, 52.5%. IR (Nujol), $\nu(CO)/cm^{-1}$: 2077, 1720; $\nu(CN)/cm^{-1}$: 2276w. 1H NMR (250 MHz, $CDCl_3$): δ 2.91 (3H, s, $COCH_3$), 6.12 (1H, m), 6.52 (1H, m), 6.70 (1H, m) ($NCCHCH_2$).

4.7. Synthesis of $[Rh(CO)(COMe)I_2(NCCH_2-CHCH_2)]_2$ (**3d**)

$[Rh(CO)_2I_2]$ (**1**) (0.5 g, 0.87 mmol) was dissolved in allyl cyanide/MeI (10 cm^3 , 5:1 v/v) and stirred at room

temperature under N_2 (48 h). Removal of the solvent in vacuo gave an orange powder which was recrystallised from a minimum volume of warm CH_2Cl_2 to give orange microcrystals of **3d**. Concentration of the solution and recrystallisation at -36 °C gave a further crop of crystals; yield: 0.665 g (77%). *Anal.* Calc. for $C_7H_8I_2NO_2Rh$: C, 17.0; H, 1.6; N, 2.8; I, 51.3. Found: C, 17.0; H, 1.6; N, 2.6; I, 51.1%. IR (Nujol), $\nu(CO)/cm^{-1}$: 2082, 1726; $\nu(CN)/cm^{-1}$: 2312w. 1H NMR (250 MHz, $CDCl_3$): δ 2.87 (3H, s, $COCH_3$), 3.65 (2H, m), 5.52 (1H, m), 5.80 (2H, m) ($NCCH_2CHCH_2$).

4.8. Synthesis of $[Rh(CO)(COMe)I_2(NC_5H_5)]_2$ (**3e**)

$[Rh(CO)_2I_2]$ (**1**) (0.35 g, 0.61 mmol) was dissolved in nitromethane/MeI (60 cm^3 , 2:1 v/v) and stirred at room temperature under N_2 (6 h). The volatile portion of the solvent was removed and pyridine (0.1 cm^3 , 1.24 mmol) was added to the remainder. The reaction mixture was stirred for a further 20 min and the resulting orange solid collected by filtration. Further reduction of the filtrate in vacuo gave a second crop of orange powder. The combined product was recrystallised from CH_2Cl_2 at 0 °C to give two crops of small red-brown crystals; yield: 0.38 g (61%). *Anal.* Calc. for $C_8H_8I_2NO_2Rh$: C, 19.0; H, 1.6; N, 2.8; I, 50.1. Found: C, 19.4; H, 1.5; N, 2.8; I, 49.7%. IR (Nujol), $\nu(CO)/cm^{-1}$: 2085, 1718. 1H NMR (250 MHz, $CDCl_3$): δ 2.95 (3H, s, $COCH_3$), 7.31 (2H, m), 7.85 (1H, m), 9.52 (2H, m) (NC_5H_5).

4.9. Synthesis of $[Rh_2(CO)_2(COMe)_2I_4(NC(CH_2)_4-CN)]$ (**4**)

Adiponitrile (0.02 g, 0.18 mmol) was added to a solution of $[Rh(CO)_2I_2]$ (**1**) (0.1 g, 0.175 mmol) in CH_2Cl_2/MeI (6 cm^3 , 2:1 v/v) under N_2 . The stirred solution was heated to reflux for 3 h and on cooling a dark red powder was formed, which was collected by filtration. Reduction of the filtrate in vacuo gave a further crop of red powder. The product was sparingly soluble in most solvents but could be recrystallised from warm nitromethane or nitrobenzene. The resulting dark red crystals were collected by filtration; yield: 0.1 g (59%). *Anal.* Calc. for $C_6H_7I_2NO_2Rh$: C, 15.0; H, 1.5; N, 2.9; I, 52.7. Found: C, 15.4; H, 1.7; N, 2.7; I, 53.3%. IR (Nujol), $\nu(CO)/cm^{-1}$: 2079, 1715; $\nu(CN)/cm^{-1}$: 2300w, 2249vw. 1H NMR (250 MHz, $C_6D_5NO_2$): δ 3.05 (3H, $COCH_3$).

4.10. Synthesis of $[Rh(CO)(COMe)I_2(NC_5H_5)]_2$ (**6e**)

$[Rh(CO)_2I_2]$ (**1**) (0.35 g, 0.61 mmol) was dissolved in nitromethane/MeI (60 cm^3 , 2:1 v/v) and stirred at room temperature under N_2 (6 h). The volatile portion of the

solvent was removed and pyridine (0.2 cm³, 2.48 mmol) was added to the remainder. The reaction mixture was stirred for a further 5 min and the volatile portion of the solvent removed in vacuo. The solution was filtered (Hiflo), concentrated, and cooled to –30 °C to give a crop of dark red crystals which were collected by filtration; yield: 0.58 g (81%). *Anal.* Calc. for C₁₃H₁₃I₂N₂O₂Rh: C, 26.7; H, 2.2; N, 4.8; I, 43.3. Found: C, 26.8; H, 2.4; N, 4.3; I, 43.4%. IR (Nujol), $\nu(\text{CO})/\text{cm}^{-1}$: 2079, 1716. ¹H NMR (250 MHz, CDCl₃): δ 3.10 (3H, s, COCH₃), 7.26 (4H, m), 7.77 (2H, m), 8.83 (2H, m), 9.21 (2H, m) (2×NC₅H₅).

4.11. Synthesis of [Rh(dppe)(COMe)I₂] (**7a**) [21,22]

The diphosphine dppe (0.1 mmol) was dissolved, together with complex **3a** (0.085 g, 0.2 mmol) in CH₂Cl₂ (20 cm³). The solution was warmed to a gentle reflux and after 1 h had turned from red to orange-yellow in colour. Diethyl ether was added, and after 24 h at –10 °C, the product was recovered by filtration as a yellow-brown precipitate; yield: 85%. *Anal.* Calc. for C₂₈H₂₇I₂OP₂Rh: C, 42.1; H, 3.4; I, 31.8. Found: C, 42.1; H, 3.4; I, 31.8%. IR (CH₂Cl₂), $\nu(\text{CO})/\text{cm}^{-1}$: 1712. ³¹P NMR (CD₂Cl₂): δ 70.1 (d, ¹J_{Rh-P} 139 Hz).

4.12. Synthesis of [Rh(dppp)(COMe)I₂] (**7b**) [21,23,24]

The method described above for **7a** was used; yield: 78%. *Anal.* Calc. for C₂₉H₂₉I₂OP₂Rh: C, 42.9; H, 3.6; I, 31.3. Found: C, 43.0; H, 3.6; I, 31.3%. IR (CH₂Cl₂), $\nu(\text{CO})/\text{cm}^{-1}$: 1701. ³¹P NMR (CD₂Cl₂): δ 17.9 (d, ¹J_{Rh-P} 132 Hz).

4.13. Synthesis of [Rh(dppb)(COMe)I₂] (**7b**)

The method described above for **7a** was used; yield: 63%. *Anal.* Calc. for C₃₀H₃₁I₂OP₂Rh: C, 42.9; H, 3.6; I, 31.3. Found: C, 43.3; H, 3.6; I, 30.9%. IR (CH₂Cl₂), $\nu(\text{CO})/\text{cm}^{-1}$: 1702. ³¹P NMR (CD₂Cl₂): δ 72.1 (d, ¹J_{Rh-P} 136 Hz).

4.14. X-ray structure determinations

Three dimensional, room temperature X-ray data were collected in the range 3.5° < 2θ < 50° on a Nicolet R3 4-circle diffractometer by the omega scan method. The independent reflections (1610 of 2167 measured for **3a**; 1622 of 2672 measured for **3b**) for which $|F|/\sigma(|F|) > 3.0$ were corrected for Lorentz and polarisation effects and for absorption by analysis of 8 azimuthal scans (minimum and maximum transmission coefficients 0.028 and 0.051 for **3a** and 0.109 and 0.145 for **3b**). The structures were solved by Patterson and Fourier techniques and refined by blocked cascade least squares methods. Hydrogen atoms were included in

calculated positions with isotropic thermal parameters related to those of the supporting atom, and refined in riding mode.

Crystal data for [Rh(CO)(NCMe)(COMe)(I)(μ-I)]₂ (**3a**): C₁₀H₁₂I₄N₂O₄Rh₂; *M* = 937.64; the complex crystallised from a solution in warm dichloromethane as dark red elongated blocks with crystal dimensions of 0.45 × 0.25 × 0.20 mm. Monoclinic, *a* = 7.470(4) Å, *b* = 11.242(7) Å, *c* = 13.444(9) Å, β = 104.13(5)°, *U* = 1094.8(12) Å³; *D*_{calc} = 2.844 g cm⁻³, *Z* = 2. Space group *P*2₁/*n* (a non-standard setting of *P*2₁/*c*, *C*_{2h}⁵, No. 14), Mo Kα radiation (λ = 0.71069 Å), μ(Mo Kα) = 70.81 cm⁻¹, *F*(000) = 839.95. Refinement converged at a final *R* = 0.0544 (100 parameters, maximum δ/σ 0.001) with allowance for the thermal anisotropy of all non-hydrogen atoms. A final difference electron density synthesis showed minimum and maximum values of –1.02 and +1.10 e Å⁻³. Complex scattering factors were taken from [49] and from the program package SHELXTL [50] as implemented on the Data General Nova 3 computer. A weighting scheme with $w^{-1} = [\sigma^2(F) + 0.00143(F)^2]$ was used in the latter stages of the refinement. CCDC 228895.

Crystal data for [Rh(CO)(NC^tBu)(COMe)(I)(μ-I)]₂ (**3b**): C₁₆H₂₄I₄N₂O₄Rh₂; *M* = 1021.80; the complex crystallised from a solution in warm dichloromethane containing a drop of ^tbutyl cyanide as red needles with crystal dimensions of 0.425 × 0.20 × 0.20 mm. Triclinic, *a* = 7.223(14) Å, *b* = 10.449(37) Å, *c* = 11.165(38) Å, α = 66.93(26)°, β = 75.68(22)°, γ = 83.43(23)°, *U* = 751(4) Å³; *D*_{calc} = 2.259 g cm⁻³, *Z* = 1. Space group *P* $\bar{1}$ (*C*_i¹, No. 2) Mo Kα radiation (λ = 0.71069 Å), μ(Mo Kα) = 51.71 cm⁻¹, *F*(000) = 467.97. Refinement converged at a final *R* = 0.0698 (*R*_w 0.0669, 127 parameters; mean and maximum δ/σ both 0.000) with allowance for the thermal anisotropy of all non-hydrogen atoms. A final difference electron density synthesis showed minimum and maximum values of –2.23 and +0.97 e Å⁻³. Complex scattering factors were taken from [49] and from the program package SHELXTL [50] as implemented on the Data General Nova 3 computer. A weighting scheme with $w^{-1} = [\sigma^2(F) + 0.00071(F)^2]$ was used in the latter stages of the refinement. CCDC 228894.

The atomic positional parameters, anisotropic thermal vibration parameters, hydrogen atom positional parameters and the observed structure amplitudes and calculated structure factors (with estimated standard deviations) for both complexes are supplied as Supplementary information.

4.15. Kinetic experiments

Pseudo-first-order conditions were employed, with at least a 100-fold excess of MeI, relative to the metal complex. The required amount of freshly distilled MeI was placed in a 10 cm³ graduated flask, which was then made up to the mark with the solvent of choice (usually

MeCN). A portion of this solution was used to record a background spectrum. A second portion (5 cm³) was added to the reactant complex **1** (typically 15 mg) in a graduated flask to give a reaction solution containing ca. 10 mM [Rh]. Alternatively, an appropriate quantity of MeI was added to a solution of [Ir(CO)₂(NCMe)I], generated by the reaction of Ph₄As[Ir(CO)₂I₂] with a slight excess of InI₃ in MeCN. A portion of the reaction solution was quickly transferred to the IR cell and the kinetic experiment was started. The IR cell (0.5 mm pathlength, CaF₂ windows) was maintained at constant temperature throughout the kinetic run by a thermostated jacket. Spectra were recorded in the $\nu(\text{CO})$ region (2200–1600 cm⁻¹) and saved at regular time intervals under computer control. After the kinetic run, absorbance versus time data for the appropriate $\nu(\text{CO})$ frequencies were extracted and analysed off-line using Kaleidagraph software. Observed rate constants were reproducible ($\pm 5\%$) and reported values are mean values of two or more runs.

Acknowledgements

This work was supported by BP Chemicals Ltd. (studentships to I.A.S. and J.M.P.; PDRF to S.H.), EPSRC and the University of Sheffield.

References

- [1] M.J. Howard, M.D. Jones, M.S. Roberts, S.A. Taylor, *Catal. Today* 18 (1993) 325.
- [2] P.M. Maitlis, A. Haynes, G.J. Sunley, M.J. Howard, *J. Chem. Soc., Dalton Trans.* (1996) 2187.
- [3] N. Yoneda, S. Kusano, M. Yasui, P. Pujado, S. Wilcher, *Appl. Catal. A* 221 (2001) 253.
- [4] F.E. Paulik, J.F. Roth, *Chem. Commun.* (1968) 1578.
- [5] M.J. Howard, G.J. Sunley, A.D. Poole, R.J. Watt, B.K. Sharma, *Stud. Surf. Sci. Catal.* 121 (1999) 61.
- [6] J.H. Jones, *Platinum Metals Rev.* 44 (2000) 94.
- [7] A. Haynes, *Educ. Chem.* 38 (2001) 99.
- [8] G.J. Sunley, D.J. Watson, *Catal. Today* 58 (2000) 293.
- [9] D. Forster, *Adv. Organomet. Chem.* 17 (1979) 255.
- [10] T.W. Dekleva, D. Forster, *Adv. Catal.* 34 (1986) 81.
- [11] A. Haynes, B.E. Mann, D.J. Gulliver, G.E. Morris, P.M. Maitlis, *J. Am. Chem. Soc.* 113 (1991) 8567.
- [12] A. Haynes, B.E. Mann, G.E. Morris, P.M. Maitlis, *J. Am. Chem. Soc.* 115 (1993) 4093.
- [13] M. Bassetti, D. Monti, A. Haynes, J.M. Pearson, I.A. Stanbridge, P.M. Maitlis, *Gazz. Chim. Ital.* 122 (1992) 391.
- [14] P.R. Ellis, J.M. Pearson, A. Haynes, H. Adams, N.A. Bailey, P.M. Maitlis, *Organometallics* 13 (1994) 3215.
- [15] J.M. Pearson, A. Haynes, G.E. Morris, G.J. Sunley, P.M. Maitlis, *J. Chem. Soc., Chem. Commun.* (1995) 1045.
- [16] T. Ghaffar, H. Adams, P.M. Maitlis, G.J. Sunley, M.J. Baker, A. Haynes, *Chem. Commun.* (1998) 1023.
- [17] A. Haynes, P.M. Maitlis, G.E. Morris, G.J. Sunley, H. Adams, P.W. Badger, C.M. Bowers, D.B. Cook, P.I.P. Elliott, T. Ghaffar, H. Green, T.R. Griffin, M. Payne, J.M. Pearson, M.J. Taylor, P.W. Vickers, R.J. Watt, *J. Am. Chem. Soc.* 126 (2004) 2847.
- [18] G.W. Adamson, J.J. Daly, D. Forster, *J. Organomet. Chem.* 71 (1974) C17.
- [19] D. Forster, *J. Am. Chem. Soc.* 98 (1976) 846.
- [20] H. Adams, N.A. Bailey, B.E. Mann, C.P. Manuel, C.M. Spencer, A.G. Kent, *J. Chem. Soc., Dalton Trans.* (1988) 489.
- [21] K.G. Moloy, R.W. Wegman, *Organometallics* 8 (1989) 2883.
- [22] L. Gonsalvi, H. Adams, G.J. Sunley, E. Ditzel, A. Haynes, *J. Am. Chem. Soc.* 124 (2002) 13597.
- [23] I. Sötofte, J. Hjortkjaer, *Acta Chem. Scand.* 48 (1994) 872.
- [24] K.G. Moloy, J.L. Petersen, *Organometallics* 14 (1995) 2931.
- [25] A. Adams, N.A. Bailey, B.E. Mann, C.P. Manuel, *Inorg. Chim. Acta* 198–200 (1992) 111.
- [26] A. Fulford, P.M. Maitlis, *J. Organomet. Chem.* 366 (1989) C20.
- [27] D. Forster, *Inorg. Chem.* 8 (1969) 2556.
- [28] L.F. Dahl, C. Martell, D.L. Wampler, *J. Am. Chem. Soc.* 83 (1961) 1761.
- [29] D. Roberto, E. Cariati, R. Psaro, R. Ugo, *Organometallics* 13 (1994) 4227.
- [30] R. Ugo, F. Bonati, M. Fiore, *Inorg. Chim. Acta* 2 (1968) 463.
- [31] B.T. Heaton, C. Jacob, T. Sampanthar, *J. Chem. Soc., Dalton Trans.* (1998) 1403.
- [32] L. Gonsalvi, J.A. Gaunt, H. Adams, A. Castro, G.J. Sunley, A. Haynes, *Organometallics* 22 (2003) 1047.
- [33] V.G. Albano, P. Chini, S. Martinengo, M. Sansoni, D. Strumolo, *J. Chem. Soc., Chem. Commun.* (1974) 299.
- [34] G.A. Olah, T.E. Kiovsk, *J. Am. Chem. Soc.* 90 (1968) 4666.
- [35] D. Forster, *J. Am. Chem. Soc.* 97 (1975) 951.
- [36] A. Fulford, C.E. Hickey, P.M. Maitlis, *J. Organomet. Chem.* 398 (1990) 311.
- [37] T.R. Griffin, D.B. Cook, A. Haynes, J.M. Pearson, D. Monti, G.E. Morris, *J. Am. Chem. Soc.* 118 (1996) 3029.
- [38] E.A. Ivanova, P. Gisdakis, V.A. Nasluzov, A.I. Rubailo, N. Rösch, *Organometallics* 20 (2001) 1161.
- [39] T. Kinnunen, K. Laasonen, *J. Mol. Struct. (Theochem)* 542 (2001) 273.
- [40] M. Cheong, R. Schmid, T. Ziegler, *Organometallics* 19 (2000) 1973.
- [41] R. Ettorre, *Inorg. Nucl. Chem. Lett.* 5 (1969) 45.
- [42] P.W. Hall, R.J. Puddephatt, C.F.H. Tipper, *J. Organomet. Chem.* 84 (1975) 407.
- [43] P.K. Byers, A.J. Canty, M. Crespo, R.J. Puddephatt, J.D. Scott, *Organometallics* 7 (1988) 1363.
- [44] A.J. Canty, *Acc. Chem. Res.* 25 (1992) 83.
- [45] K.I. Goldberg, J.Y. Yan, E.L. Winter, *J. Am. Chem. Soc.* 116 (1994) 1573.
- [46] K.I. Goldberg, J.Y. Yan, E.M. Breitung, *J. Am. Chem. Soc.* 117 (1995) 6889.
- [47] A. Haynes, P.R. Ellis, P.K. Byers, P.M. Maitlis, *Chem. Br.* 28 (1992) 517.
- [48] J. McCleverty, G. Wilkinson, *Inorg. Synth.* 8 (1966) 214.
- [49] *International Tables for X-ray Crystallography*, vol. 4, Kynoch Press, Birmingham, 1974.
- [50] G.M. Sheldrick, *SHELXTL: An Integrated System for Solving, Refining and Displaying Crystal Structures from Diffraction Data (Revision 4)*, University of Gottingen, Gottingen, Germany, 1983.